Effect of Fractional Fluorination on the Properties of ATRP Surface-Initiated Poly(hydroxyethyl methacrylate) Films

Mayker R. Bantz,[‡] Eric L. Brantley,[‡] Randy D. Weinstein,[†] Jeffrey Moriarty,[†] and G. Kane Jennings*[,‡]

Department of Chemical Engineering, Vanderbilt University, Nashville, Tennessee 37235, and Department of Chemical Engineering, Villanova University, Villanova, Pennsylvania 19085

Received: February 18, 2004; In Final Form: April 27, 2004

Acylation of a surface-initiated poly(hydroxyethyl methacrylate) (PHEMA) film with a perfluoroalkyl acid chloride ($C_7F_{15}COCl$) results in a highly blocking film with fluorocarbon side groups that orient at the air−film interface to produce an ultralow-energy surface. The kinetics of the acylation step was monitored with reflectance-absorption infrared spectroscopy to reveal that the rate of fluorination depends on the chain length and solution concentration of the perfluorinated acid chloride as well as the solvent used. By control of the time of exposure to $C_7F_{15}COCl$, films with fractional conversion of the hydroxyl groups to fluorinated esters between 0 and 0.8 were produced. Increasing fractional conversion from 0 to ∼0.2 has a dramatic effect on surface wettability and electrochemical barrier properties as a densely packed, oriented fluorocarbon surface region is formed that greatly reduces water and ion transport. Additional fluorination has no effect on wettability but gradually increases film resistance while lowering film capacitance. These results suggest that structuring of fluorocarbon groups at the outermost surface of the film has a major impact on film properties and establish the minimum content of fluorocarbon groups required to achieve the structured interface via this grafting process.

Introduction

Partially fluorinated polymer films have widespread applications in superhydrophobic and oleophobic materials,[1,2] environmentally responsive surfaces,[3,4] and protective barrier films.[5] In these applications, the fluorocarbon groups are primarily used to modify surface properties and/or act as a barrier against transport. Therefore, achieving a high level of control over both surface and bulk film composition can be important for utilizing these films in a particular application. Partially fluorinated polymer films are typically prepared by synthesizing the polymer in solution and then casting or spin-coating the film onto a support.[3,4,6,7] Subsequent curing then leads to preferential partitioning of the fluorocarbon groups to the air−film interface. While these approaches provide a high level of control over the fluorocarbon content of the polymer, they often produce weakly adhered, physically adsorbed films and do not allow good control over film thickness. In addition, these methods are not ideally suited to prepare patternable, ultrathin polymer films and structures that have enormous potential in advanced materials processing. The ability to grow fluorinated polymer films and structures from an underlying surface can circumvent many or all of these problems and is compatible with bottom-up processing. Recently explored methods to grow fluorocarbon-containing films include chemical vapor deposition[8,9] and surface-initiated polymerization of fluorinated monomers.[1]

We have recently reported a method to prepare partially fluorinated ultrathin polymer films onto a gold surface.[10] We first use water-accelerated atom transfer radical polymerization (ATRP) to grow poly(hydroxyethyl methacrylate) (PHEMA) films from an initiator modified gold surface, analogous to the method of Bruening, Baker, and co-workers.[11] Next, we acylate the reactive hydroxyl side chains of PHEMA with a perfluorinated acid chloride (C_6F_5COCl, C_3F_7COCl, or $C_7F_{15}COCl$) to produce fluorinated ester groups along the polymer backbone.[10] This modification enables high conversions (∼70−85%) of the hydroxyl side groups to fluorinated esters, depending on the packing parameter of the fluorocarbon. We have used this two-step route to a partially fluorinated film because (1) the water-accelerated growth of PHEMA results in rapid film kinetics, offers good control over thickness from a few nanometers to ∼1 μm, and produces robust, surface-anchored polymer chains on surfaces of any geometry,[11] (2) modification of PHEMA films with hydrocarbon[11] or fluorocarbon[10,12] acid chlorides is straightforward, (3) these fluorocarbon groups can be easily cleaved by exposure to base,[10] which presents opportunities for rapidly patterning hydrophobic and hydrophilic regions of polymer, (4) the general method is compatible with soft lithography[13] to potentially generate unique, partially fluorinated films and structures, and (5) the system allows the fundamental study of the effect of fluorocarbon chain length, composition, and conversion on film and surface properties.

These fluorinated PHEMA films exhibited dramatically altered surface and barrier properties in comparison with PHEMA. In fact, the critical surface tension for C_7F_{15}−PHEMA (9 mN/m) is even lower than that of Teflon (18 mN/m) due to the dominance of CF_3 groups at the outer surface for C_7F_{15}−PHEMA.[10] The barrier properties also improved greatly as the resistance to charge transfer increased ∼10 000-fold and the capacitance decreased ∼100 fold. We also observed that the longer-chain C_7F_{15}− side group structures the film to a greater extent than the shorter chained C_3F_7− analogue whereas the

* To whom all correspondence should be addressed. E-mail: jenningk@vuse.vanderbilt.edu. Fax: 615-343-7951.
† Villanova University.
‡ Vanderbilt University.

10.1021/jp049255f CCC: $27.50
Published on Web 06/08/2004

C_6F_5- side group likely $\pi-\pi$ stacks within the film and produces the best barrier properties of the films examined.[10]

This initial work examined solely initial and final state properties of the films and did not address the dynamics of the fluorination process. Important unresolved issues include the rate at which the fluorinated acid chlorides penetrate the film to acylate the hydroxyl side chains and the effect of fractional conversion of hydroxyl groups to fluorinated esters on film and surface properties. A unique advantage of this two-step approach of surface-initiated ATRP and subsequent modification is that it enables the straightforward preparation of films with controlled extents of fluorination and, based on diffusion of reactants into the film, may also allow for depth-dependent fluorination. The ability to produce ultrathin films where fluorination occurs only at or near the surface could be useful in multifunctional films and in economically driven applications where surface properties are much more important than bulk film properties.

The results presented herein detail our efforts to understand the time dependence of fluorination of PHEMA and the effect of conversion on film and surface properties. We use reflectance-absorption infrared spectroscopy (RAIRS) to characterize the film structure and composition; contact angle measurements to qualitatively assess the surface composition of the film, electrochemical impedance spectroscopy (EIS) to determine the effectiveness of the films as barriers against the transport of redox species, and ellipsometry to quantify the expansion of the film upon fluorination. Effects of variables such as exposure time and the concentration and chain length of the perfluorinated acid chloride were examined to gain a greater understanding of the dynamics of this process in order to prepare films with prescribed properties.

Experimental Section

Materials. Gold shot (99.99%) and chromium-coated tungsten filaments were obtained from J&J Materials and R. D. Mathis, respectively. Silicon (100) wafers (Montco Silicon) were rinsed with ethanol and deionized water and dried with nitrogen immediately prior to use. Copper(I) chloride (99.995+%), copper(II) bromide (99.999%), $K_3Fe(CN)_6$ (99+%), $K_4Fe(CN)_6 \cdot 3H_2O$ (99%), 2,2′-dipyridyl (bpy, 99%), 2-hydroxyethyl methacrylate (HEMA, >99%), pentadecafluorooctanoyl chloride (97%), heptafluorobutyryl chloride (98%), and hexadecane were used as received from Aldrich. *N*,*N*-Dimethylformamide (DMF, 99.9%), tetrahydrofuran (THF), acetone, methylene chloride (CH_2Cl_2, 99.9%), and Na_2SO_4 (anhydrous) were used as received from Fisher. Grade 5 carbon dioxide was used as received from BOC Gases. Deionized water (16.7 MΩ) was purified with a Modu-Pure system. Ethanol (EtOH, 200 proof) was used as received from Aaper. A disulfide initiator, $(BrC(CH_3)_2COO(CH_2)_{11}S)_2$, was prepared according to a literature procedure.[13]

Preparation of Gold Substrates. Gold substrates were prepared by evaporating chromium (100 Å) and gold (1250 Å) in sequence onto silicon (100) wafers at rates of $1-2$ Å s^{-1} in a diffusion-pumped chamber with a base pressure of 4×10^{-6} Torr. The wafers were typically cut into 1 cm × 3 cm or 1.5 cm × 4.5 cm pieces and rinsed thoroughly with ethanol prior to use.

Preparation of Initiator-Terminated Monolayers. Initiator-terminated monolayers were formed on gold substrates by immersing the substrate in a 1 mM solution of $(BrC(CH_3)_2COO(CH_2)_{11}S)_2$ in ethanol for 24 h. Substrates were then rinsed with ethanol and dried using nitrogen.

Preparation of PHEMA Films. Synthesis of PHEMA films on the gold surface was carried out by ATRP according to the procedure of Huang et al.[11] The initiated samples were placed in vials that were subsequently degassed and back-filled with nitrogen. A Cu^I/Cu^{II}/bpy (69 mM CuCl, 20 mM $CuBr_2$, 195 mM bpy) system in a 50:50 v:v water/HEMA solution[11] was used for polymerization. Since a glovebox was not available and oxygen will oxidize the activating Cu^I species and terminate polymerization, the mixture was placed in a Schlenk flask sealed with a rubber septum and was degassed by performing three freeze−pump−thaw cycles. The mixture was then transferred via cannula into vials containing up to six samples each. After being polymerized for 12 h at room temperature, the samples were thoroughly rinsed with water and DMF and then dried with nitrogen. PHEMA film thicknesses were 270 ± 20 nm under these conditions.[10]

Preparation of Fluorinated PHEMA. The PHEMA films were then acylated by immersion into 3, 8, or 30 mM solutions of C_3F_7COCl or $C_7F_{15}COCl$ in CH_2Cl_2 or other solvents for varying periods of time between 3 min and 24 h. Upon removal, the samples were rinsed with fresh solvent and ethanol and dried using nitrogen. Preparation in pressurized carbon dioxide was done using a reactor system and procedures described previously.[14]

Reflectance-Absorption Infrared Spectroscopy (RAIRS). Reflectance-absorption IR spectra of polymer-coated gold surfaces were obtained in single reflection mode using a Bio-Rad Excalibur FTS-3000 infrared spectrometer equipped with a Universal Sampling Accessory. The polarized light was incident on the sample at 80° from the surface normal. Reflected light was detected with a narrow-band MCT detector cooled with liquid nitrogen. Spectral resolution was 2 cm^{-1} after triangular apodization. The spectra were referenced against a gold sample containing a SAM prepared from octadecanethiol-d_{37}, and 1000 scans were accumulated on all samples. The reported spectra are representative of more than six spectra accumulated under the same conditions with each sample prepared independently.

IR spectra were used to estimate conversion (χ) of the PHEMA film by acylation based on the integrated OH absorbance ($A_{OH,t}$) at 3100−3700 cm^{-1} [10]

$$\chi = 1 - \frac{A_{OH,t}}{A_{OH,t=0}} \tag{1}$$

which assumes that any decrease in OH absorbance scales directly with the hydroxyl group concentration in the film.

Wetting Measurements. Advancing and receding contact angle measurements on static drops of water and hexadecane were obtained using a Rame-Hart goniometer. An attached syringe supplied by Rame-Hart was used to advance or retreat the contacting liquids prior to measurement of the angle. The syringe tip remained in the drop during the advancing/retreating of the contacting liquid and the angle measurement. Measurements were taken on both sides of the contacting liquid on one location on a sample. Reported values and error bars represent the averages and standard deviations, respectively, of contact angles measured on at least three different samples prepared independently.

Electrochemical Impedance Spectroscopy (EIS). Electrochemical impedance spectra of the polymer-coated gold working electrodes were obtained using a Gamry Instruments CMS300 electrochemical impedance system interfaced with a personal computer. A gold-coated silicon counter electrode, a Ag/AgCl/saturated KCl reference electrode, and an aqueous solution of

TABLE 1. Conversion upon Exposure of 270 nm PHEMA Films to 8 mM $C_7F_{15}COCl$ for 24 h in the Following Solvents

solvent	conversion	comments
CH_2Cl_2	~80%	best, most consistent solvent
acetone	0%	solubilized reagents; no reaction
THF	<10%	poor solvation of acid chlorides
DMF	<20%	poor solvation of acid chlorides
CO_2	0−80%	results irreproducible

0.1 M Na_2SO_4, 1 mM $K_3Fe(CN)_6$, and 1 mM $K_4Fe(CN)_6 \cdot 3H_2O$ were used in a flat cell (Princeton Applied Research) so that the area of the working electrode was confined to 1 cm^2 and sample edges were not exposed to electrolyte. Film resistance and capacitance values were determined by fitting the EIS data with appropriate equivalent circuit models using software provided by Gamry. Reported values and error bars represent the averages and standard deviations, respectively, of resistance or capacitance measured on at least three different samples prepared independently.

Ellipsometry. Ellipsometry measurements were taken on a J. A. Woollam Co. M-2000DI variable angle spectroscopic ellipsometer with WVASE32 software for modeling. Measurements at three spots per sample were taken with light incident at a 75° angle from the surface normal using wavelengths from 250 to 1000 nm with the refractive index assumed to be 1.5 at all wavelengths. While 1.5 is higher than the index of refraction for purely fluorocarbon films (1.37),[15] use of values less than 1.5 yielded inferior fits to the data by the modeling software. We also attempted to use more complex models containing up to two Cauchy layers (one for a PHEMA-rich layer and one for a C_7F_{15}-rich layer), with optical constant and thickness fits for each layer, but this method was plagued by poor fits and inconsistencies across a series of films. Optical constants of a bare gold sample were determined by ellipsometry and used as the baseline from which all polymer film samples were measured. Film thickness of the polymer layer present on samples, regardless of modification, was fit to a Cauchy layer model with the refractive index set to 1.5. Reported thickness values and error bars represent the mean and standard deviation of three measurements at separate points along the surface of the sample.

Results and Discussion

Effect of Solvent on Acylation of PHEMA Films. To examine the effect of solvent on the acylation of PHEMA films, we exposed 270-nm PHEMA films to 8 mM solutions of $C_7F_{15}COCl$ in various solvents for 24 h and estimated the conversion (χ) by eq 1 (Table 1). A good solvent for this process must be able to solvate the fluorocarbon acid chloride reactants and swell both partially and extensively fluorinated PHEMA to facilitate molecular diffusion of the reactants into the film to acylate the hydroxyl side chains. *N*,*N*-Dimethylformamide (DMF) was previously used as solvent for acylation of PHEMA with low molecular weight hydrocarbon acid chlorides by Huang et al.,[11] but we found that fluorocarbon acid chlorides precipitated out of solution, producing nonuniform conversion across a sample. Tetrahydrofuran (THF) as solvent produced similar results with the acid chloride precipitating out of solution. While both DMF and THF can swell PHEMA,[16] neither of these solvents can solvate the fluorocarbon acid chloride well or swell the partially fluorinated film. Acetone appeared to solvate the acid chloride completely, based on the clear appearance of the solution, but no compositional changes were produced in the PHEMA film. We also explored the use of liquid (25 °C, 100−300 bar) and supercritical (35 °C, 100−300 bar) carbon dioxide as solvents because of their environmental friendliness and strong solvating ability of fluorocarbons.[17] While high conversions ($\chi = \sim 0.8$) were occasionally obtained in liquid CO_2, the results were largely irreproducible with typical conversions of ~0.05 even though the acid chlorides were soluble in carbon dioxide (up to at least 50 mM) over the temperature and pressure range explored. Dichloromethane (CH_2Cl_2) proved to be the best solvent examined for this process, effectively solubilizing the acid chlorides and giving consistently high conversion. Dichloromethane is sufficiently polar to swell PHEMA[16] and appears to be sufficiently fluorophilic to swell the partially fluorinated film to provide diffusional access for additional reagent. Because of these favorable properties, we used dichloromethane as solvent in all subsequent experiments reported herein.

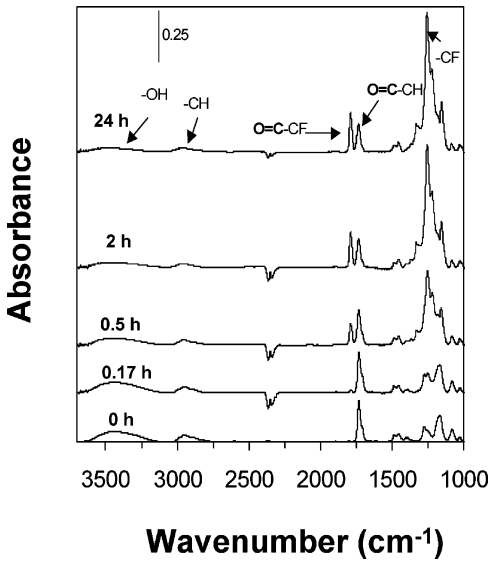

Figure 1. Reflectance-absorption infrared spectra of 270 nm PHEMA films on gold after exposure to 8 mM $C_7F_{15}COCl$ in CH_2Cl_2 for the indicated times. There are several key regions of interest when evaluating the extent of the acylation reaction: C−F stretching, 1100−1400 cm^{-1}; C═O stretching, 1700−1800 cm^{-1}; and O−H stretching, 3100−3700 cm^{-1}.

The remainder of this paper is divided into two parts; the first part focuses on the kinetics of acylation of PHEMA films while the second part examines how the conversion of hydroxyl side groups to fluorinated esters affects surface and barrier properties of the films. In the first part, we use reflectance-absorption IR spectra to assess compositional and structural changes of the films during acylation and to calculate the conversion of the hydroxyl side chains within the polymer films. In the second part, we use wetting and impedance measurements to monitor surface and barrier properties as a function of conversion to elucidate the effect of fluorination on film properties.

Time Dependence of Film Fluorination. Figure 1 shows reflectance-absorption IR spectra of PHEMA films after exposure to 8 mM solutions of $C_7F_{15}COCl$ in dichloromethane at different time intervals up to 24 h. The initial spectrum of PHEMA shows broad bands due to hydroxyl stretching (3100−3700 cm^{-1}) and C−H stretching (2840−3000 cm^{-1}) and sharper peaks for carbonyl stretching (1733 cm^{-1}) and C−O stretching at 1276, 1252, and 1167 cm^{-1}.[10,11,18] During the reaction process, PHEMA undergoes a nucleophilic acyl substitution and elimination of HCl as $-C(O)C_7F_{15}$ side chains are incorporated into the polymer film. Factors indicative of fluorination are (1) the appearance of strong absorbance in the C−F stretching region

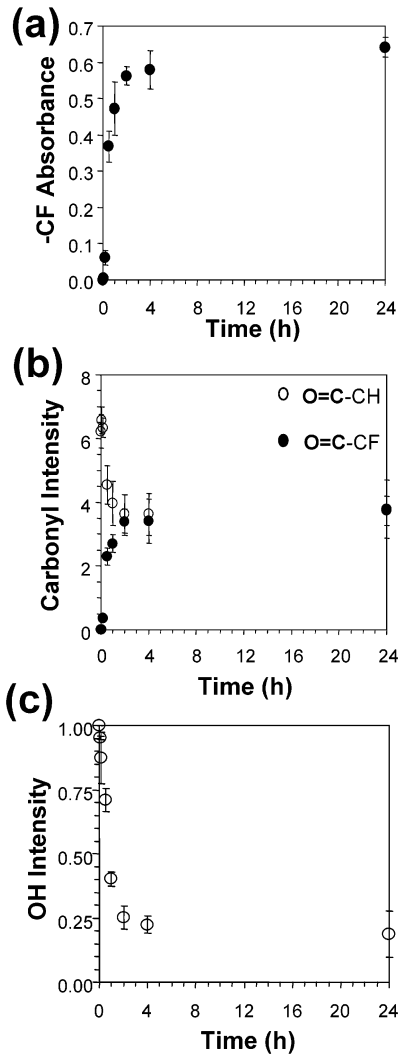

Figure 2. Time dependence of (a) C−F absorbance, (b) carbonyl intensities, and (c) normalized hydroxyl intensity, obtained from reflectance-absorption infrared spectra of 270 nm PHEMA films on gold upon exposure to 8 mM $C_7F_{15}COCl$ in CH_2Cl_2.

from 1100 to 1400 cm^{-1}, (2) the appearance of a second carbonyl peak at 1790 cm^{-1} due to the addition of the fluorinated ester, and (3) the diminution of hydroxyl (−OH) stretching peaks as the alcohol groups are converted to esters.[10]

The time-dependent IR spectra shown in Figure 1 provide compositional information as the film becomes increasingly fluorinated. From 0 to 0.17 h, the film undergoes only minor changes, the most noticeable being the slight appearance of C−F stretching bands at 1252 cm^{-1}, the origins of a band for the second carbonyl at 1790 cm^{-1}, and a slight decrease in the hydroxyl absorbance. From 0.17 to 0.5 h, changes in peak positions indicate transition of film composition and structure toward that of a highly fluorinated C_7F_{15} film. As shown previously by Rabolt et al.[19] and later by Fukushima et al.,[20] there are two types of CF_2 stretching peaks observed in the IR: those due to transition dipole moments along the helical axis ($\upsilon_{ax}^{CF_2}$, 1400−1300 cm^{-1}) and those due to transition dipole moments perpendicular to the helical axis ($\upsilon_{pd}^{CF_2}$, 1300−1100 cm^{-1}). Specifically, from 0.17 to 0.5 h, a $\upsilon_{ax}^{CF_2}$ peak appears at 1330 cm^{-1} and a $\upsilon_{pd}^{CF_2}$ peak at 1157 cm^{-1}, both as shoulders to the dominant $\upsilon_{pd}^{CF_2}$ peak at 1252 cm^{-1}.

Noticeable increases in IR peak intensities due to CF_2 (1252 cm^{-1}) and **O═C**−CF_2−(1790 cm^{-1}) occur between 0.5 and 2 h along with a corresponding decrease in OH stretching intensity

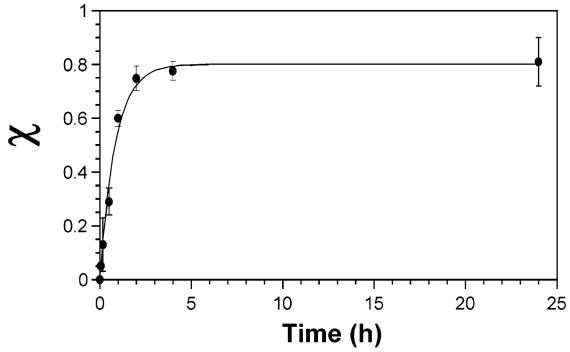

Figure 3. Time dependence of conversion of hydroxyl side groups to fluorinated esters, as measured using IR spectra and eq 1, upon exposure of 270 nm PHEMA films on gold to 8 mM $C_7F_{15}COCl$ in CH_2Cl_2. The solid curve is a fit of the data based on eq 3, where kC is estimated from the fit as 3.25×10^{-4} s^{-1}. The correlation coefficient (R^2) for the fit is 0.995.

(3100−3700 cm^{-1}) as fluorinated side groups are added into the film. During this time, the peak positions do not shift by more than 1 cm^{-1}, suggesting that there are no significant structural changes for the fluorocarbon chains as the limiting conversion is approached. From 2 to 24 h, these same peaks in the spectra show little or no change in position or integrated absorbance. The lack of change in the IR spectra at long times suggests that there is little free volume for additional fluorocarbon chains to add into the film. We have theorized that steric effects prevent some hydroxyl groups from becoming acylated.[10]

To more clearly illustrate the kinetics of the fluorination, Figure 2 shows (a) C−F absorbance (at 1252 cm^{-1}), (b) **O═C**−CF_2− (1790 cm^{-1}) and **O═C**−CH_2− (1733 cm^{-1}) intensities, and (c) normalized OH (3100−3700 cm^{-1}) intensity as a function of exposure time of PHEMA to 8 mM $C_7F_{15}COCl$ in dichloromethane. The intensities of all these modes achieve an approximately asymptotic limit after 2 h of exposure as hydroxyl groups are converted to fluorinated esters. In Figure 2b, the **O═C**−CF_2− intensity increases as a function of time while the PHEMA carbonyl (**O═C**−CH_2−) intensity decreases as a function of time. The increase of the **O═C**−CF_2− intensity is due to the acylation of the hydroxyl groups, and from Figure 1, this peak is shifted to higher wavenumbers than the peak corresponding to the carbonyl on the PHEMA side chain (1790 cm^{-1} compared to 1733 cm^{-1}) due to α-halogen substitution.[10] We have concluded that the decrease in the **O═C**−CH_2− intensity is due to orientational effects during acylation as the film expands. This peak is restored to its original intensity when the sample is hydrolyzed back to PHEMA with a base.[10]

We have used the time-dependent decrease in hydroxyl stretching from Figure 2c and eq 1 to estimate conversion (χ) of the hydroxyl groups to fluorinated esters. Figure 3 shows that χ reaches an upper limit of ∼0.8. Exposure of PHEMA to $C_7F_{15}COCl$ solutions at very high concentrations (80 mM) for several days did not yield conversions greater than ∼0.8. At the limiting conversion, the film likely has no accessible hydroxyl groups for the fluorinated acid chlorides to react and further fluorinate the film.

To obtain quantitative kinetics information for acylation of PHEMA with $C_7F_{15}COCl$, the conversion data in Figure 3 were fit with a simplest-case model, which assumes that the rate is proportional to the concentrations of the fluorinated acid chloride in solution (C) and accessible −OH groups within the film:

$$\frac{d\chi}{dt} = kC(\chi_f - \chi) \qquad (2)$$

or, upon integration,

$$\chi = \chi_f(1 - e^{-kCt}) \quad (3)$$

where t is time and χ_f is the limiting conversion (~0.8). Use of eq 3 provides a good fit to the transient conversion data in Figure 3 (correlation coefficient = $R^2 = 0.995$) and enables an estimate of kC as 3.25×10^{-4} s^{-1}.

The close correlation between eq 3 and the kinetics data provides a strong argument that this simplest case model is suitable to obtain rate data for comparing chain length and concentration effects on the kinetics of acylation and that the extensive calculations that otherwise would be required to model the system rigorously are unnecessary. For example, a rigorous solution must allow for the changing film composition, which affects the diffusion coefficient of the acid chloride within the film, the volumetric expansion of the film due to addition of fluorocarbon groups, and the time and spatial dependences on species concentration. Such a rigorous solution would require solving a system of coupled, partial differential equations consisting of unsteady conservation equations for both the acid chloride and hydroxyl sites, a kinetics equation to describe the acylation reaction, and an equation to allow for the changing volume of the film as fluorination occurs. Such a solution would be computationally exhaustive and, to our knowledge, has never been reported.

To assess the effect of solution concentration on the kinetics of acylation, we monitored the time dependence of conversion at $C_7F_{15}COCl$ concentrations of 3, 8, and 30 mM in CH_2Cl_2 using RAIRS and eq 3 (Figure 4a). In each case after 24 h, similar conversions of ~0.8 are achieved, indicating no concentration effect on the limiting conversion. The $C_7F_{15}COCl$ concentration did affect the kinetics of acylation with the higher concentrations, producing a more rapid initial increase in conversion. The data sets were fit with eq 3 to determine values for kC at each concentration, which is then plotted against C in Figure 4b. The high degree of linearity in Figure 4b ($R^2 = 0.999$) indicates that the kinetics of acylation exhibits a first-order dependence on solution concentration and agrees with assumptions of eq 3. From the slope of the line, k is 42 cm^3/mol s.

We also investigated the effect of the chain length of the fluorinated acid chloride on the kinetics of acylation to assess the extent of diffusional effects on the process. Figure 5 shows conversion as a function of time upon exposure of 270 nm thick PHEMA films to 8 mM C_3F_7COCl or 8 mM $C_7F_{15}COCl$. The C_3F_7-modified PHEMA film reaches the asymptotic conversion more rapidly than does C_7F_{15}−PHEMA, exhibiting a k of 180 cm^3/mol s, which is ~4.3 times greater than that for C_7F_{15}−PHEMA. This faster approach to the limiting conversion for the smaller reactant indicates that fluorocarbon chain length plays a role in the kinetics of acylation but not in determining the ultimate conversion. The more rapid kinetics of C_3F_7COCl is possibly due to its less constrained diffusion within the film and/or the fact that C_3F_7-modified PHEMA chains at the outer surface of the film would provide less of a diffusional barrier than C_7F_{15}-modified PHEMA would.[10] Regardless of the reason, this result suggests that diffusion of reactants into the film does affect the rate of acylation, consistent with the widely varying results obtained using different solvents (Table 1). The insensitivity of the limiting conversion on chain length and the fact that we have obtained higher conversions for perfluoroaryl acid chlorides[10] with a flat, disklike shape suggest that the van der Waals diameter of the fluorocarbon molecule (and not its length) affects the limiting conversion, consistent with steric limitations along a common backbone.

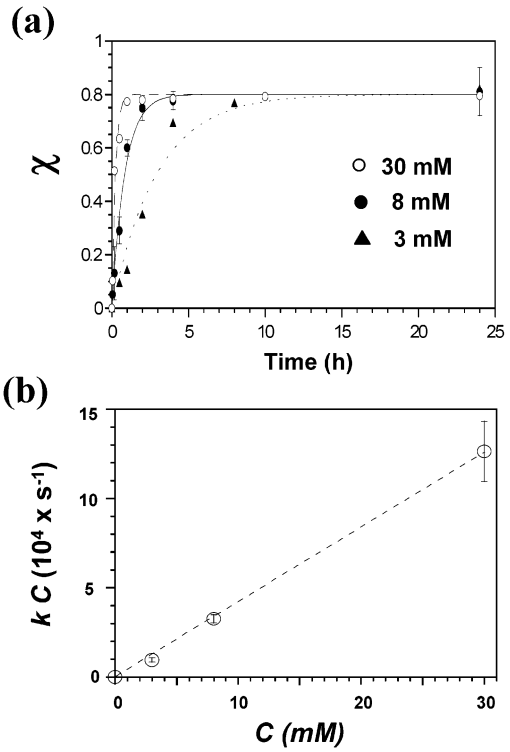

Figure 4. (a) Effect of $C_7F_{15}COCl$ concentration in CH_2Cl_2 on the time dependence of conversion of a 270 nm thick PHEMA film on gold. The solid curves are fits of the data based on eq 3. The correlation coefficients for the fits are 0.985, 0.995, and 0.987 for 3, 8, and 30 mM, respectively. (b) kC, as estimated from the fits of the data in part a with eq 3, as a function of $C_7F_{15}COCl$ solution concentration to assess whether the process is first order. The correlation coefficient for the line is 0.999. From the fit, k is estimated as 42 cm^3/mol s. The error bars in part b are determined by the estimate in error of kC based on the fits from part a.

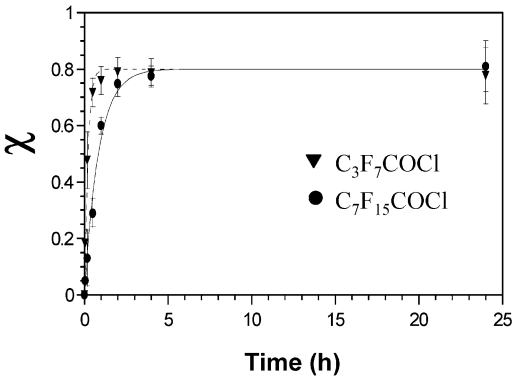

Figure 5. Time dependence of conversion of hydroxyl side groups to fluorinated esters, as measured using IR spectra and eq 1, upon exposure of 270 nm PHEMA films on gold to 8 mM solutions of $C_7F_{15}COCl$ or C_3F_7COCl in CH_2Cl_2. The curves are fits of the data based on eq 3, where kC values are estimated from the fits as 3.25×10^{-4} and 1.44×10^{-3} s^{-1} for $C_7F_{15}COCl$ and C_3F_7COCl, respectively. The correlation coefficients for these fits are 0.995 and 0.998 for $C_7F_{15}COCl$ and C_3F_7COCl, respectively.

Figures 2−5 illustrate that the modification of surface-initiated polymer films to produce partially fluorinated films proceeds with rapid kinetics and produces high conversions of the polymer side groups. The use of a surface-initiated growth ensures that the polymer chains are robustly bound to the underlying metal surface, provides a means of controlling the thickness of the original film,[11] and creates the potential for directing the polymer growth on a prepatterned substrate.[13] Furthermore, the acylation of a surface-initiated film simplifies

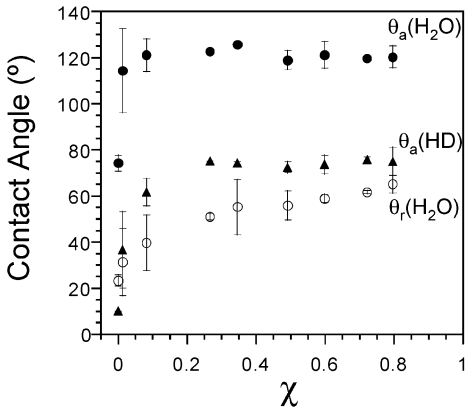

Figure 6. Effect of the fractional conversion of PHEMA to $C_7F_{15}-$PHEMA on the advancing and receding contact angles of water and the advancing contact angle of hexadecane. The receding contact angles of hexadecane (not shown for clarity) vary between 65 and 69° for $\chi \geq 0.25$. Where no error bar is visible, the error is approximated by the size of the symbol.

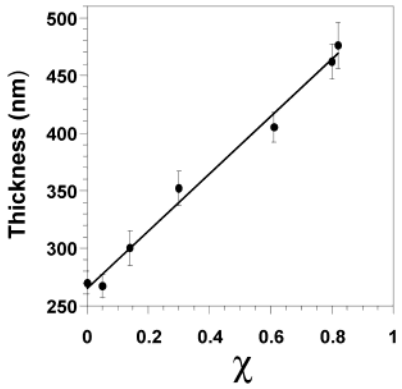

Figure 7. Effect of fractional conversion of PHEMA to $C_7F_{15}-$PHEMA on film thickness as measured by ellipsometry. The line represents a least-squares fit to the data with a correlation coefficient of 0.995.

separations as compared with a homogeneous polymerization and/or grafting. Another *potential* attribute of this methodology, explored in the next section, is the ability to control the extent of functionalization of a film to engineer the film properties for a specific purpose.

Effect of Conversion on Film Properties. In the remainder of this paper, we report the effect of conversion, modulated by changing acylation time, on film properties, including surface wettabilities, film thicknesses, and barrier properties. This work seeks to determine the extent of fluorination required to produce a dense fluorocarbon surface region vs that required to affect the resistance and capacitance of the film. Such information will provide mechanistic clues on the fluorination process and fundamental insight as to how surface and film composition affect the barrier properties of a polymer film.

Wetting Measurements. Contact angles of water (H_2O) and hexadecane (HD) were measured on all films to assess the effect of conversion on the composition at the outermost surface of the film. We used both H_2O and HD because these liquids exhibit different sensitivities to fluoroalkyl groups. While the contact angle of H_2O is greatly increased when PHEMA is acylated with a fluorocarbon acid chloride,[10] HD exhibits greater overall sensitivity to surface chemical composition[21] since it will give different contact angles on $-CF_2-$, $-CF_3$, $-CH_2-$, and $-CH_3$ surfaces[22,23] due to different levels of dispersive interaction with the surface groups. In contrast, H_2O will yield similar contact angle values on these surfaces[22,23] because it is a more polar liquid that interacts weakly with these different nonpolar groups.

Figure 6 shows the advancing and receding contact angles of H_2O and the advancing contact angles of HD as conversion is increased. The advancing contact angle of H_2O increases rapidly from 75 to ~120° during the first 10% of film conversion while that for HD more slowly reaches its asymptotic value of ~75° at $\chi = 0.25$. Dependent upon chain length, self-assembled monolayers exhibiting $-CF_3$ surfaces are known to exhibit HD contact angles from 70 to 80° while CF_2-rich polymers typically exhibit lower contact angles ($\theta_{eq} \sim 40°$).[14,24] Therefore, the measured value of 75° is consistent with $-CF_3$ groups dominating the outermost surface, indicating the outer fluorocarbon groups are oriented nearly normal to the surface. The rapid increase of $\theta_a(H_2O)$ with χ at very early conversions suggests hydrophobic material (either $-CF_2$ or $-CF_3$) is present at the surface and that the outermost surface is converted more rapidly than the bulk film. The more gradual increase of θ_a(HD) with χ indicates that the hydrophobic material at the outer surface is not dominated by $-CF_3$ groups until $\chi \cong 0.25$ and is consistent with the heightened sensitivity of HD for CF_3 groups as compared with water. The insensitivity of θ_a(HD) with χ for $\chi > 0.25$ indicates that the CF_3-rich surface composition is set at low conversion and implies that the remaining fluorination occurs in the bulk of the polymer film. The large contact angle hysteresis for water ($\theta_a(H_2O) - \theta_r(H_2O)$) suggests that the films are rough, especially at low χ, but the gradual increase in $\theta_r(H_2O)$ (reduction in hysteresis) for $\chi > 0.25$ suggests that fluorination throughout the remainder of the film may result in a smoothing of the surface. Combined, these wetting results suggest that fluorocarbon groups are rather sparsely packed and highly canted on a rough surface at low conversion ($\chi < 0.25$) but become densely packed at $\chi \sim 0.25$, creating a CF_3-rich surface that becomes progressively smoother as conversion is increased ($\chi > 0.25$). This dense region of oriented fluorocarbon at the outermost surface is consistent with the structure of spun-cast semifluorinated polyisoprene thin films as determined by Genzer et al. using NEXAFS.[7] According to Figure 3, the kinetics of acylation are still rapid for $\chi > 0.25$, so this fluorocarbon-rich surface region does not provide a significant diffusion barrier against further acylation and may even improve the partitioning of the fluorinated acid chlorides into the film.

Ellipsometry. To assess the effect of conversion on film expansion, we used spectroscopic ellipsometry to measure film thickness at different conversions of $C_7F_{15}-$PHEMA. Figure 7 shows that film thickness increases linearly with conversion, consistent with a volumetric expansion of the film as the large fluorocarbon groups add into the film. These results are consistent with our recent work, which showed that film expansion is related closely to the molecular volume of the fluorinated acid chloride.[10] The linear expansion of the film with χ and molecular volume is consistent with a model in which the PHEMA backbone, initially in a canted and coiled state to maximize interchain interactions, becomes extended as the fluorocarbon groups add into the film.

Electrochemical Impedance Spectroscopy. We have recently shown that modification of PHEMA with $C_7F_{15}COCl$ greatly increases film resistance and lowers film capacitance,[10] consistent with a thicker, more hydrophobic medium that reduces free volume for ion-conducting pathways. In the present work, we used EIS to examine the effect of conversion on the film barrier properties upon exposure to 1 mM $K_3Fe(CN)_6$ and 1 mM $K_4Fe(CN)_6$ in 0.1 M Na_2SO_4(aq). Figure 8 shows EIS

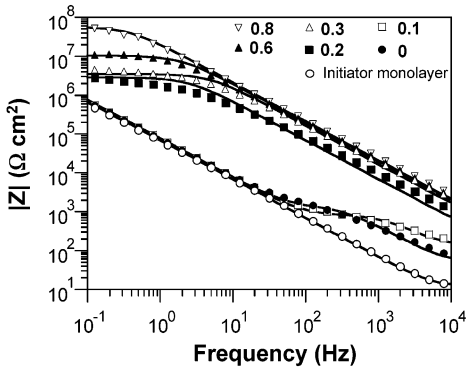

Figure 8. Electrochemical impedance spectra obtained in 1 mM $K_3Fe(CN)_6$ and 1 mM $K_4Fe(CN)_6$ in 0.1 M Na_2SO_4(aq). Spectra are shown for PHEMA and various conversions of C_7F_{15}−PHEMA with initiator-modified gold shown for reference. Solid curves represent fits of the data to equivalent circuit models (see text).

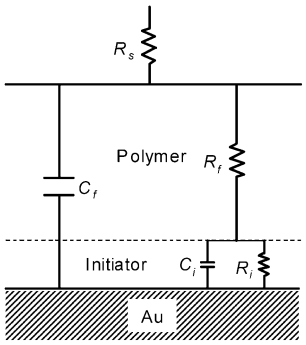

Figure 9. Equivalent circuit used to model impedance spectra for polymer films on gold. For PHEMA films and modified films at low conversion ($\chi < 0.10$), both time constants (one due to initiator and one due to the polymer film) appear in the impedance spectrum. For modified films with $\chi > 0.10$, the impedance due to R_f is much greater than the combined impedance of R_i and C_i in parallel, so the time constant due to the initiator is not observed in the impedance spectra. For these cases, the equivalent circuit simplifies to a Randles model with R_f and C_f in parallel with one another but in series with R_s.

spectra in the form of Bode plots for gold modified progressively with the disulfide initiator, PHEMA, and selected conversions of C_7F_{15}-modified PHEMA. The solid curves in Figure 8 represent best fits of the data based on appropriate equivalent circuit models to provide quantitative information on the effect of conversion on the resistance and capacitance of the films. The impedance spectrum for the initiator-terminated self-assembled monolayer is fit with a parallel combination of initiator resistance (R_i) and capacitance (C_i) in series with solution resistance (R_s), which is identical in form to the Randles model that is commonly used to fit impedance spectra for monolayers on metal surfaces.[25−27]

For the case of a PHEMA film ($\chi = 0$), a more complex model shown in Figure 9 provides an appropriate fit. This more complex circuit contains a time constant due to the initiator ($\tau_i = R_iC_i$) and one due to the polymer film ($\tau_f = R_fC_f$). The contribution of PHEMA is limited to the time constant at high frequencies, as discussed recently by us.[10] The PHEMA layer reduces total film capacitance (C_f) due to its enhanced thickness (270 nm) but exhibits very low resistance (R_f) compared to that of the initiator-terminated monolayer (R_i). The low resistance of PHEMA is indicative of a loosely packed, poor barrier film, which allows water and ions to easily permeate through the film. Nonetheless, the poor barrier properties of PHEMA are advantageous for the preparation of partially fluorinated films since a larger molecule (such as the fluorinated acid chlorides) can

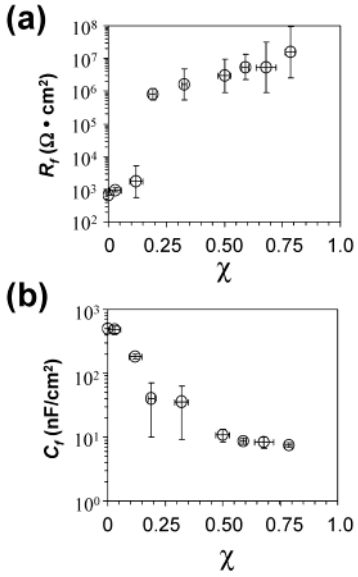

Figure 10. Effect of fractional conversion of PHEMA to C_7F_{15}−PHEMA on (a) polymer film resistance (R_f) and (b) film capacitance (C_f). Resistance and capacitance values were obtained by fitting impedance spectra with an appropriate equivalent circuit model (see text).

effectively diffuse into the film and react with side chains throughout the film.

Upon fluorination at low conversion ($\chi \leq 0.1$), the impedance data show two time constants, similar to the spectrum of PHEMA and yielding analogous interpretation. The only difference in these spectra is a higher impedance at highest frequencies for $\chi = 0.1$, which is consistent with a reduced capacitance (490 vs 640 nF/cm^2) of the partially converted film as hydrophobic fluorocarbon groups replace hydrophilic hydroxyl moieties. For higher conversion ($\chi > 0.10$), the time constant due to the initiator monolayer cannot be observed because the resistance due to the polymer (R_f) becomes significantly greater than the combined impedance corresponding to the initiator monolayer. Upon neglect of R_i and C_i in Figure 9, the equivalent circuit model therefore simplifies to a modified Randles model where R_f and C_f are easily obtained.

R_f and C_f values are shown as a function of χ in Figure 10, parts a and b, respectively. R_f does not increase measurably at the lowest conversions ($\chi \sim 0.1$) but increases by 3 orders of magnitude from ~0.1 to ~0.2, yielding an R_f value approaching 1 MΩ cm^2 (Figure 10a). C_f decreases by a factor of 5 over this same range (Figure 10b). This dramatic increase in R_f and decrease in C_f from ~0.1−0.2 approximately corresponds to the same conversion range ($\chi \leq 0.25$) at which the hexadecane contact angle achieves its asymptotic value (Figure 6), which suggests that the structuring of fluorocarbon groups within the outer region of the film dramatically affects barrier properties. This dense fluorocarbon region likely inhibits the penetration of aqueous ions into the film to greatly improve the film resistance while lowering the effective dielectric constant as compared with a more permeable, unmodified PHEMA film.

R_f increases more gently (from ~1 to ~15 MΩ cm^2) as χ is increased from 0.2 to 0.75 whereas C_f decreases from 40 to 8 nF/cm^2 over this same range. These significant, but more gradual, changes are consistent with an expansion of the polymer due to fluorination in the bulk of the film, further lowering the effective dielectric constant and reducing ion-diffusing pathways to boost the time constant for the film. The more dramatic changes in R_f and C_f at low χ, combined with wetting properties

in Figure 6, suggest that a highly fluorinated surface region in contact with the aqueous solution provides an important contribution to film resistance. Nonetheless, to obtain films and coatings with superior blocking properties, the highest conversions must be achieved.

Conclusions

By focusing on the dynamics of the acylation of PHEMA with perfluorinated acid chlorides, we have developed several important conclusions regarding both the kinetics of film fluorination and the effect of fluorocarbon groups on film properties. First, dichloromethane is a suitable solvent that solvates the fluorocarbon acid chloride and swells both partially and extensively fluorinated PHEMA to facilitate the diffusion of the acid chloride molecules into the film for modification. The kinetics of film fluorination depends directly on the solution concentration of the acid chloride and the concentration of unreacted hydroxyl groups within the film; however, diffusional effects are still important.

These kinetics results also illustrate that controlling the time of exposure for PHEMA films with the perfluorinated acid chlorides can be used to produce films with different conversions. At low conversion ($\chi \sim 0.1$), hydrophobic groups are present at the surface but are not structured. For $\chi \sim 0.25$, fluorocarbon groups become structured to produce an oleophobic surface that is dominated by CF_3 groups. This densely packed fluorocarbon surface region seems to greatly improve barrier properties. Additional fluorination ($0.25 \leq \chi \leq 0.8$) has no effect on surface wettability but does continually expand the film and increase film resistance while lowering capacitance.

Acknowledgment. We gratefully acknowledge the National Science Foundation (CTS-0203183 and a Graduate Research Fellowship (E.L.B.)) for financial support.

References and Notes

(1) Jung, D. H.; Park, I. J.; Choi, Y. K.; Lee, S. B.; Park, H. S.; Ruhe, J. *Langmuir* **2002**, *18*, 6133−6139.

(2) Lau, K. K. S.; Bico, J.; Teo, K. B. K.; Chhowalla, M.; Amaratunga, G. A. J.; Milne, W. I.; McKinley, G. H.; Gleason, K. K. *Nano Lett.* **2003**, *3*, 1701−1705.

(3) Vaidya, A.; Chaudhury, M. K. *J. Colloid Interface Sci.* **2002**, *249*, 235−245.

(4) Thanawala, S. K.; Chaudhury, M. K. *Langmuir* **2000**, *16*, 1256−1260.

(5) Zhao, M.; Zhou, Y.; Bruening, M. L.; Bergbreiter, D. E.; Crooks, R. M. *Langmuir* **1997**, *13*, 1388−1391.

(6) Ravenstein, L. v.; Ming, W.; Grampel, R. D. v. d.; Linde, R. v. d.; With, G. d.; Loontjens, T.; Thune, P. C.; Niemantsverdriet, J. W. *Macromolecules* **2004**, *37*, 408−413.

(7) Genzer, J.; Sivaniah, E.; Kramer, E. J.; Wang, J. G.; Korner, H.; Xiang, M. L.; Char, K.; Ober, C. K.; DeKoven, B. M.; Bubeck, R. A.; Chaudhury, M. K.; Sambasivan, S.; Fischer, D. A. *Macromolecules* **2000**, *33*, 1882−1887.

(8) Lau, K. K. S.; Murthy, S. K.; Lewis, H. G. P.; Caulfield, J. A.; Gleason, K. K. *J. Fluorine Chem.* **2003**, *122*, 93−96.

(9) Murthy, S. K.; Olsen, B. D.; Gleason, K. K. *J. Appl. Polym. Sci.* **2004**, *91*, 2176−2185.

(10) Brantley, E. L.; Jennings, G. K. *Macromolecules* **2004**, *37*, 1476−1483.

(11) Huang, W.; Kim, J.-B.; Bruening, M. L.; Baker, G. L. *Macromolecules* **2002**, *35*, 1175−1179.

(12) Balachandra, A. M.; Baker, G. L.; Bruening, M. L. *J. Membr. Sci.* **2003**, *227*, 1−14.

(13) Shah, R. R.; Merreceyes, D.; Husemann, M.; Rees, I.; Abbott, N. L.; Hawker, C. J.; Hedrick, J. L. *Macromolecules* **2000**, *33*, 597−605.

(14) Weinstein, R. D.; J. Moriarty; Cushnie, E.; R. Colorado, J.; Lee, T. R.; Patel, M.; Alesi, W. R.; Jennings, G. K. *J. Phys. Chem. B* **2003**, *107*, 11626−11632.

(15) Sandrin, L.; Silverstein, M. S.; Sacher, E. *Polymer* **2001**, *42*, 3761−3769.

(16) Brandrup, J.; Immergut, E. H.; Grulke, E. A. *Polymer Handbook*; 4th ed.; Wiley: New York, 1989.

(17) DeSimone, J. M.; Guan, Z.; Elsbernd, C. S. *Science* **1996**, *275*, 945.

(18) Silverstein, R. M.; Webster, F. X. *Spectrometric Identification of Organic Compounds*; 6th ed.; Wiley: New York, 1998.

(19) Tsao, W.-W.; Hoffman, C. L.; Rabolt, J. F.; Johnson, H. E.; Castner, D. G.; Erdelen, C.; Ringsdorf, H. *Langmuir* **1997**, *13*, 4317−4322.

(20) Fukushima, H.; Seki, S.; Nishikawa, T.; Takiguchi, H.; Tamada, K.; Abe, K.; Colorado, R.; Graupe, M.; Shmakova, O. E.; Lee, T. R. *J. Phys. Chem. B* **2000**, *104*, 7417−7423.

(21) Laibinis, P. E.; Bain, C. D.; Nuzzo, R. G.; Whitesides, G. M. *J. Phys. Chem.* **1995**, *99*, 7663−7676.

(22) Laibinis, P. E.; Palmer, B. J.; Lee, S.-W.; Jennings, G. K. The Synthesis of Organothiols and their Assembly into Monolayers on Gold. In *Thin Films*, Ulman, A., Ed.; Academic Press: San Diego, CA, 1998; Vol. 24, pp 1−41, and references therein.

(23) Graupe, M.; Takenaga, M.; Koini, T.; R. Colorado, J.; Lee, T. R. *J. Am. Chem. Soc.* **1999**, *121*, 3222−3223.

(24) Janczuk, B.; Bialopiotrowicz, T.; Zdziennicka, A. *J. Colloid Interface Sci.* **1999**, *211*, 96−103.

(25) Nahir, T. M.; Bowden, E. F. *Electrochim. Acta* **1994**, *39*, 2347−2352.

(26) Barbour, E.; Lennox, R. B. *Langmuir* **2000**, *16*, 4222−4228.

(27) Jennings, G. K.; Munro, J. C.; Yong, T.-H.; Laibinis, P. E. *Langmuir* **1998**, *14*, 6130−6139.